

See discussions, stats, and author profiles for this publication at: <https://www.researchgate.net/publication/236163189>


Advances in FDTD Computational Electrodynamics: Photonics and Nanotechnology

Book · January 2013

CITATIONS
70

READS
2,106

3 authors, including:



Allen Taflove

Northwestern University

203 PUBLICATIONS 28,029 CITATIONS

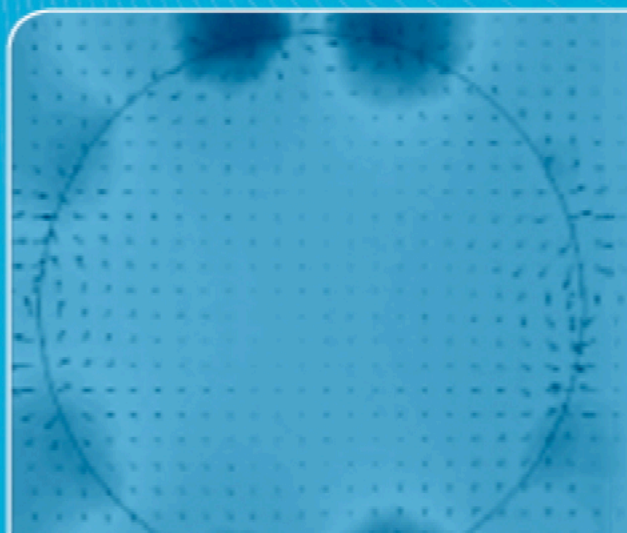
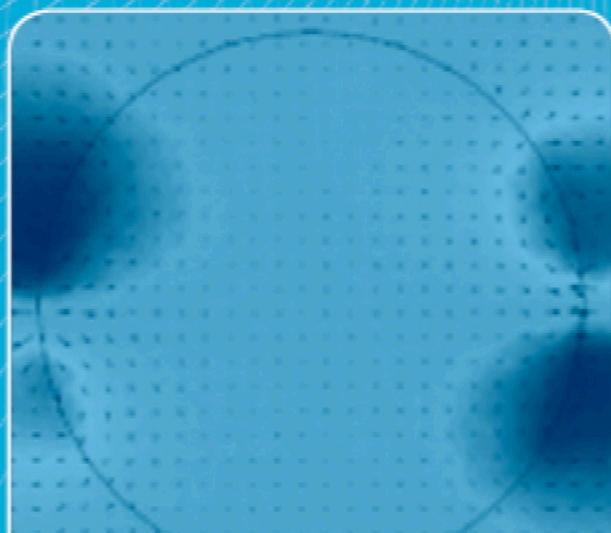
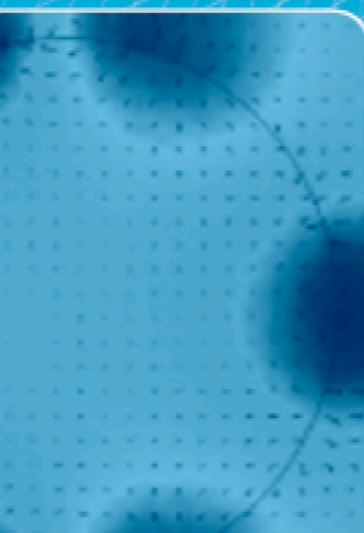
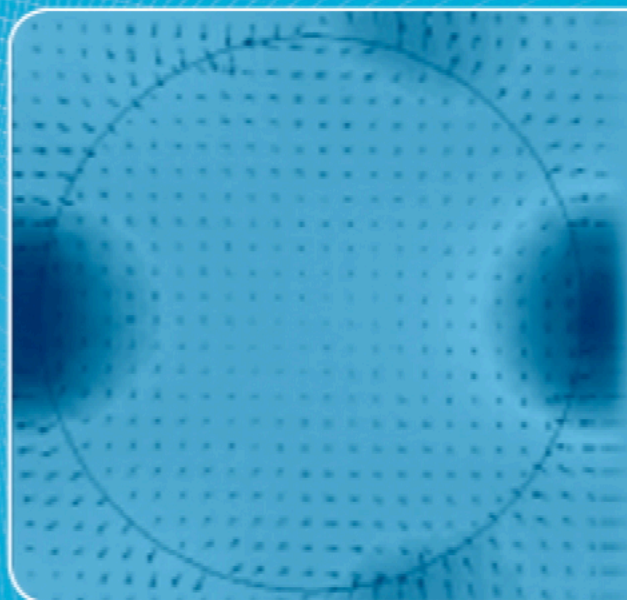
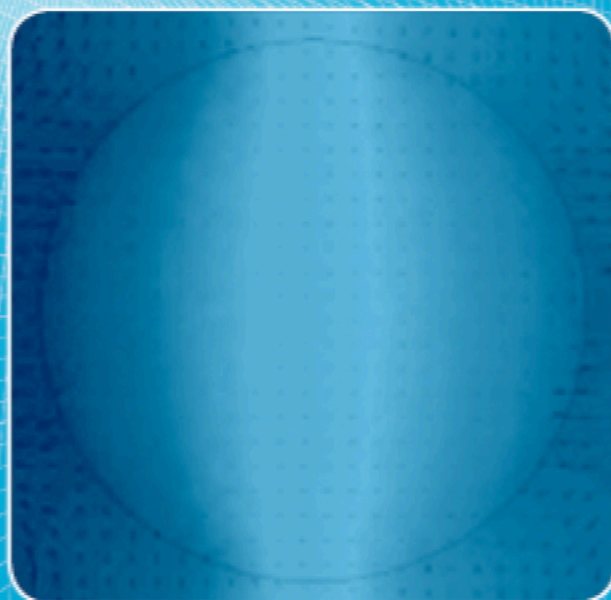
SEE PROFILE

Advances in FDTD Computational Electrodynamics

Photonics and Nanotechnology

Allen Taflove, Editor

Ardavan Oskooi and **Steven G. Johnson**, Coeditors



Contents

Preface

xv

1 Parallel-Processing Three-Dimensional Staggered-Grid Local-Fourier-Basis PSTD Technique

Ming Ding and Kun Chen

1

1.1	Introduction	1
1.2	Motivation	1
1.3	Local Fourier Basis and Overlapping Domain Decomposition	3
1.4	Key Features of the SL-PSTD Technique	4
1.4.1	FFT on a Local Fourier Basis	4
1.4.2	Absence of the Gibbs Phenomenon Artifact	7
1.5	Time-Stepping Relations for Dielectric Systems	7
1.6	Elimination of Numerical Phase Velocity Error for a Monochromatic Excitation	9
1.7	Time-Stepping Relations within the Perfectly Matched Layer Absorbing Outer Boundary	10
1.8	Reduction of the Numerical Error in the Near-Field to Far-Field Transformation	13
1.9	Implementation on a Distributed-Memory Supercomputing Cluster	14
1.10	Validation of the SL-PSTD Technique	16
1.10.1	Far-Field Scattering by a Plane-Wave-Illuminated Dielectric Sphere	16
1.10.2	Far-Field Radiation from an Electric Dipole Embedded within a Double-Layered Concentric Dielectric Sphere	18
1.11	Summary	19
	References	20

2 Unconditionally Stable Laguerre Polynomial-Based FDTD Method

Bin Chen, Yantao Duan, and Hailin Chen

21

2.1	Introduction	21
2.2	Formulation of the Conventional 3-D Laguerre-Based FDTD Method	22
2.3	Formulation of an Efficient 3-D Laguerre-Based FDTD Method	26
2.4	PML Absorbing Boundary Condition	30
2.5	Numerical Results	33
2.5.1	Parallel-Plate Capacitor: Uniform 3-D Grid	33
2.5.2	Shielded Microstrip Line: Graded Grid in One Direction	35
2.5.3	PML Absorbing Boundary Condition Performance	37
2.6	Summary and Conclusions	38
	References	39

3 Exact Total-Field/Scattered-Field Plane-Wave Source Condition

Tengmeng Tan and Mike Potter

41

3.1	Introduction	41
3.2	Development of the Exact TF/SF Formulation for FDTD	43
3.3	Basic TF/SF Formulation	43
3.4	Electric and Magnetic Current Sources at the TF/SF Interface	44
3.5	Incident Plane-Wave Fields in a Homogeneous Background Medium	45
3.6	FDTD Realization of the Basic TF/SF Formulation	46

3.7	On Constructing an Exact FDTD TF/SF Plane-Wave Source	48
3.8	FDTD Discrete Plane-Wave Source for the Exact TF/SF Formulation	49
3.9	An Efficient Integer Mapping	52
3.10	Boundary Conditions and Vector Plane-Wave Polarization	55
3.11	Required Current Densities \mathbf{J}_{inc} and \mathbf{M}_{inc}	56
3.12	Summary of Method	59
3.13	Modeling Examples	59
3.14	Discussion	62
	References	62

4 Electromagnetic Wave Source Conditions

	<i>Ardavan Oskooi and Steven G. Johnson</i>	65
4.1	Overview	65
4.2	Incident Fields and Equivalent Currents	65
4.2.1	The Principle of Equivalence	66
4.2.2	Discretization and Dispersion of Equivalent Currents	69
4.3	Separating Incident and Scattered Fields	70
4.4	Currents and Fields: The Local Density of States	73
4.4.1	The Maxwell Eigenproblem and the Density of States	74
4.4.2	Radiated Power and the Harmonic Modes	75
4.4.3	Radiated Power and the LDOS	78
4.4.4	Computation of LDOS in FDTD	78
4.4.5	Van Hove Singularities in the LDOS	80
4.4.6	Resonant Cavities and Purcell Enhancement	81
4.5	Efficient Frequency-Angle Coverage	83
4.6	Sources in Supercells	86
4.7	Moving Sources	89
4.8	Thermal Sources	92
4.9	Summary	95
	References	96

5 Rigorous PML Validation and a Corrected Unsplit PML for Anisotropic Dispersive Media

	<i>Ardavan Oskooi and Steven G. Johnson</i>	101
5.1	Introduction	101
5.2	Background	102
5.3	Complex Coordinate Stretching Basis of PML	103
5.4	Adiabatic Absorbers and PML Reflections	104
5.5	Distinguishing Correct from Incorrect PML Proposals	105
5.6	Validation of Anisotropic PML Proposals	106
5.7	Time-Domain PML Formulation for Terminating Anisotropic Dispersive Media	108
5.8	PML Failure for Oblique Waveguides	110
5.9	Summary and Conclusions	112
	Acknowledgments	112
	Appendix 5A: Tutorial on the Complex Coordinate-Stretching Basis of PML	112
5A.1	Wave Equations	113
5A.2	Complex Coordinate Stretching	114
5A.3	PML Examples	118
5A.4	PML in Inhomogeneous Media	120
5A.5	PML for Evanescent Waves	121

Appendix 5B: Required Auxiliary Variables	122
Appendix 5C: PML in Photonic Crystals	123
5C.1 Conductivity Profile of the pPML	123
5C.2 Coupled-Mode Theory	124
5C.3 Convergence Analysis	125
5C.4 Adiabatic Theorems in Discrete Systems	126
5C.5 Toward Better Absorbers	126
References	128
Selected Bibliography	132
 6 Accurate FDTD Simulation of Discontinuous Materials by Subpixel Smoothing	 133
<i>Ardavan Oskooi and Steven G. Johnson</i>	
6.1 Introduction	133
6.2 Dielectric Interface Geometry	134
6.3 Permittivity Smoothing Relation, Isotropic Interface Case	134
6.4 Field Component Interpolation for Numerical Stability	135
6.5 Convergence Study, Isotropic Interface Case	136
6.6 Permittivity Smoothing Relation, Anisotropic Interface Case	139
6.7 Convergence Study, Anisotropic Interface Case	140
6.8 Conclusions	142
Acknowledgment	143
Appendix 6A: Overview of the Perturbation Technique Used to Derive Subpixel Smoothing	143
References	147
 7 Stochastic FDTD for Analysis of Statistical Variation in Electromagnetic Fields	 149
<i>Steven M. Smith and Cynthia M. Furse</i>	
7.1 Introduction	149
7.2 Delta Method: Mean of a Generic Multivariable Function	150
7.3 Delta Method: Variance of a Generic Multivariable Function	151
7.4 Field Equations	154
7.5 Field Equations: Mean Approximation	155
7.6 Field Equations: Variance Approximation	156
7.6.1 Variance of the H -Fields	156
7.6.2 Variance of the E -Fields	157
7.7 Sequence of the Field and σ Updates	160
7.8 Layered Biological Tissue Example	161
7.9 Summary and Conclusions	164
Acknowledgment	164
References	164
 8 FDTD Modeling of Active Plasmonics	 167
<i>Iftikhar Ahmed, Eng Huat Khoo, and Er Ping Li</i>	
8.1 Introduction	167
8.2 Overview of the Computational Model	168
8.3 Lorentz-Drude Model for Metals	168
8.4 Direct-Bandgap Semiconductor Model	170
8.5 Numerical Results	174

8.5.1 Amplification of a 175-fs Optical Pulse in a Pumped Parallel-Plate Waveguide	174
8.5.2 Resonance Shift and Radiation from a Passive Disk-Shaped GaAs Microcavity with Embedded Gold Nanocylinders	177
8.6 Summary	179
Appendix 8A: Critical Points Model for Metal Optical Properties	179
Appendix 8B: Optimized Staircasing for Curved Plasmonic Surfaces	181
References	182
Selected Bibliography	183
9 FDTD Computation of the Nonlocal Optical Properties of Arbitrarily Shaped Nanostructures	185
<i>Jeffrey M. McMahon, Stephen K. Gray, and George C. Schatz</i>	
9.1 Introduction	185
9.2 Theoretical Approach	187
9.3 Gold Dielectric Function	189
9.4 Computational Considerations	191
9.5 Numerical Validation	191
9.6 Application to Gold Nanofilms (1-D Systems)	193
9.7 Application to Gold Nanowires (2-D Systems)	197
9.8 Application to Spherical Gold Nanoparticles (3-D Systems)	200
9.9 Summary and Outlook	202
Acknowledgments	203
Appendix 9A: Nonlocal FDTD Algorithm	203
References	205
10 Classical Electrodynamics Coupled to Quantum Mechanics for Calculation of Molecular Optical Properties: An RT-TDDFT/FDTD Approach	209
<i>Hanning Chen, Jeffrey M. McMahon, Mark A. Ratner, and George C. Schatz</i>	
10.1 Introduction	209
10.2 Real-Time Time-Dependent Density Function Theory	211
10.3 Basic FDTD Considerations	213
10.4 Hybrid Quantum Mechanics/Classical Electrodynamics	213
10.5 Optical Property Evaluation for a Particle-Coupled Dye Molecule for Randomly Distributed Incident Polarization	214
10.6 Numerical Results 1: Scattering Response Function of a 20-nm-Diameter Silver Nanosphere	216
10.7 Numerical Results 2: Optical Absorption Spectra of the N3 Dye Molecule	219
10.7.1 Isolated N3 Dye Molecule	219
10.7.2 N3 Dye Molecule Bound to an Adjacent 20-nm Silver Nanosphere	220
10.8 Numerical Results 3: Raman Spectra of the Pyridine Molecule	222
10.8.1 Isolated Pyridine Molecule	222
10.8.2 Pyridine Molecule Adjacent to a 20-nm Silver Nanosphere	223
10.9 Summary and Discussion	227
Acknowledgment	228
References	228

11 Transformation Electromagnetics Inspired Advances in FDTD Methods

Roberto B. Armenta and Costas D. Sarris

233

11.1	Introduction	233
11.2	Invariance Principle in the Context of FDTD Techniques	234
11.3	Relativity Principle in the Context of FDTD Techniques	235
11.4	Computational Coordinate System and Its Covariant and Contravariant Vector Bases	236
11.4.1	Covariant and Contravariant Basis Vectors	236
11.4.2	Covariant and Contravariant Components of the Metric Tensor	237
11.4.3	Covariant and Contravariant Representation of a Vector	238
11.4.4	Converting Vectors to the Cartesian Basis and Vice Versa	239
11.4.5	Second-Rank Tensors in the Covariant and Contravariant Bases	239
11.5	Expressing Maxwell's Equations Using the Basis Vectors of the Computational Coordinate System	241
11.6	Enforcing Boundary Conditions by Using Coordinate Surfaces in the Computational Coordinate System	242
11.7	Connection with the Design of Artificial Materials	246
11.7.1	Constitutive Tensors of a Simple Material	246
11.7.2	Constitutive Tensors of an Artificial Material	247
11.8	Time-Varying Discretizations	249
11.9	Conclusion	252
	References	252
	Selected Bibliography	254

12 FDTD Modeling of Nondiagonal Anisotropic Metamaterial Cloaks

Naoki Okada and James B. Cole

255

12.1	Introduction	255
12.2	Stable FDTD Modeling of Metamaterials Having Nondiagonal Permittivity Tensors	256
12.3	FDTD Formulation of the Elliptic Cylindrical Cloak	256
12.3.1	Diagonalization	256
12.3.2	Mapping Eigenvalues to a Dispersion Model	258
12.3.3	FDTD Discretization	258
12.4	Modeling Results for an Elliptic Cylindrical Cloak	261
12.5	Summary and Conclusions	265
	References	265

13 FDTD Modeling of Metamaterial Structures

Costas D. Sarris

269

13.1	Introduction	269
13.2	Transient Response of a Planar Negative-Refractive-Index Lens	270
13.2.1	Auxiliary Differential Equation Formulation	270
13.2.2	Illustrative Problem	271
13.3	Transient Response of a Loaded Transmission Line Exhibiting a Negative Group Velocity	274
13.3.1	Formulation	274
13.3.2	Numerical Simulation Parameters and Results	275
13.4	Planar Anisotropic Metamaterial Grid	277
13.4.1	Formulation	278
13.4.2	Numerical Simulation Parameters and Results	278
13.5	Periodic Geometries Realizing Metamaterial Structures	280

13.6 The Sine-Cosine Method	282
13.7 Dispersion Analysis of a Planar Negative-Refractive-Index Transmission Line	284
13.8 Coupling the Array-Scanning and Sine-Cosine Methods	285
13.9 Application of the Array-Scanning Method to a Point-Sourced Planar Positive-Refractive-Index Transmission Line	287
13.10 Application of the Array-Scanning Method to the Planar Microwave “Perfect Lens”	290
13.11 Triangular-Mesh FDTD Technique for Modeling Optical Metamaterials with Plasmonic Elements	292
13.11.1 Formulation and Update Equations	292
13.11.2 Implementation of Periodic Boundary Conditions	294
13.11.3 Stability Analysis	295
13.12 Analysis of a Sub-Wavelength Plasmonic Photonic Crystal Using the Triangular-Mesh FDTD Technique	297
13.13 Summary and Conclusions	302
Acknowledgments	303
References	303
Selected Bibliography	306

14 Computational Optical Imaging Using the Finite-Difference Time-Domain Method

<i>Ilker R. Capoglu, Jeremy D. Rogers, Allen Taflove, and Vadim Backman</i>	307
14.1 Introduction	307
14.2 Basic Principles of Optical Coherence	308
14.3 Overall Structure of the Optical Imaging System	309
14.4 Illumination Subsystem	310
14.4.1 Coherent Illumination	310
14.4.2 Incoherent Illumination	311
14.5 Scattering Subsystem	317
14.6 Collection Subsystem	319
14.6.1 Fourier Analysis	320
14.6.2 Green’s Function Formalism	326
14.7 Refocusing Subsystem	330
14.7.1 Optical Systems Satisfying the Abbe Sine Condition	331
14.7.2 Periodic Scatterers	337
14.7.3 Nonperiodic Scatterers	339
14.8 Implementation Examples: Numerical Microscope Images	344
14.8.1 Letters “N” and “U” Embossed on a Thin Dielectric Substrate	344
14.8.2 Polystyrene Latex Beads	346
14.8.3 Pair of Contacting Polystyrene Microspheres in Air	348
14.8.4 Human Cheek (Buccal) Cell	349
14.9 Summary	350
Acknowledgment	350
Appendix 14A: Derivation of Equation (14.9)	350
Appendix 14B: Derivation of Equation (14.38)	351
Appendix 14C: Derivation of Equation (14.94)	352
Appendix 14D: Coherent Focused Beam Synthesis Using Plane Waves	353
References	356

15 Computational Lithography Using the Finite-Difference Time-Domain Method

Geoffrey W. Burr and Jaione Tirapu Azpiroz

365

15.1	Introduction	365
15.1.1	Resolution	366
15.1.2	Resolution Enhancement	368
15.2	Projection Lithography	370
15.2.1	Light Source	371
15.2.2	Photomask	373
15.2.3	Lithography Lens	377
15.2.4	Wafer	378
15.2.5	Photoresist	378
15.2.6	Partial Coherence	380
15.2.7	Interference and Polarization	381
15.3	Computational Lithography	384
15.3.1	Image Formation	384
15.3.2	Mask Illumination	393
15.3.3	Partially Coherent Illumination: The Hopkins Method	398
15.3.4	Image in Resist Interference	400
15.4	FDTD Modeling for Projection Lithography	401
15.4.1	Basic FDTD Framework	402
15.4.2	Introducing the Plane-Wave Input	404
15.4.3	Monitoring the Diffraction Orders	406
15.4.4	Mapping onto the Entrance Pupil	408
15.4.5	FDTD Gridding	411
15.4.6	Parallelization	412
15.5	Applications of FDTD	414
15.5.1	Electromagnetic Field Impact of Mask Topography	414
15.5.2	Making TMA More Electromagnetic-Field Aware	416
15.5.3	Hopkins Approximation	420
15.6	FDTD Modeling for Extreme Ultraviolet Lithography	423
15.6.1	EUVL Exposure System	423
15.6.2	EUV Reticle	426
15.6.3	EUVL Mask Modeling	427
15.6.4	Hybrid Technique Using Fourier Boundary Conditions	432
15.7	Summary and Conclusions	433
	Appendix 15A: Far-Field Mask Diffraction	434
	Appendix 15B: Debye's Representation of the Focusing Fields	435
	Appendix 15C: Polarization Tensor	438
	Appendix 15D: Best Focus	440
	References	442

16 FDTD and PSTD Applications in Biophotonics

Ilker R. Capoglu, Jeremy D. Rogers, César Méndez Ruiz, Jamesina J. Simpson, Snow H. Tseng, Kun Chen, Ming Ding, Allen Taflove, and Vadim Backman

451

16.1	Introduction	451
16.2	FDTD Modeling Applications	452
16.2.1	Vertebrate Retinal Rod	452
16.2.2	Angular Scattering Responses of Single Cells	453
16.2.3	Precancerous Cervical Cells	454

16.2.4	Sensitivity of Backscattering Signatures to Nanometer-Scale Cellular Changes	458
16.2.5	Modeling Mitochondrial Aggregation in Single Cells	459
16.2.6	Focused Beam Propagation through Multiple Cells	461
16.2.7	Computational Imaging and Microscopy	463
16.2.8	Detection of Nanometer-Scale z -Axis Features within HT-29 Colon Cancer Cells Using Photonic Nanojets	471
16.2.9	Assessment of the Born Approximation for Biological Media	476
16.3	Overview of Fourier-Basis PSTD Techniques for Maxwell's Equations	478
16.4	PSTD and SL-PSTD Modeling Applications	479
16.4.1	Enhanced Backscattering of Light by a Large Cluster of 2-D Dielectric Cylinders	479
16.4.2	Depth-Resolved Polarization Anisotropy in 3-D Enhanced Backscattering	481
16.4.3	Sizing Spherical Dielectric Particles in a 3-D Random Cluster	486
16.4.4	Optical Phase Conjugation for Turbidity Suppression	489
16.5	Summary	492
	References	492

17 GVADE FDTD Modeling of Spatial Solitons

<i>Zachary Lubin, Jethro H. Greene, and Allen Taflove</i>	497
17.1 Introduction	497
17.2 Analytical and Computational Background	497
17.3 Maxwell-Ampere Law Treatment of Nonlinear Optics	498
17.4 General Vector Auxiliary Differential Equation Method	501
17.4.1 Lorentz Linear Dispersion	501
17.4.2 Kerr Nonlinearity	502
17.4.3 Raman Nonlinear Dispersion	502
17.4.4 Solution for the Electric Field	504
17.4.5 Drude Linear Dispersion for Metals at Optical Wavelengths	505
17.5 Applications of GVADE FDTD to TM Spatial Soliton Propagation	506
17.5.1 Single Narrow Fundamental TM Spatial Soliton	507
17.5.2 Single Wide Overpowered TM Spatial Soliton	508
17.5.3 Interactions of Co-Propagating Narrow TM Spatial Solitons	508
17.6 Applications of GVADE FDTD to TM Spatial Soliton Scattering	511
17.6.1 Scattering by a Square Sub-Wavelength Air Hole	511
17.6.2 Interactions with Thin Plasmonic Gold Films	512
17.7 Summary	515
References	516

18 FDTD Modeling of Blackbody Radiation and Electromagnetic Fluctuations in Dissipative Open Systems

<i>Jonathan Andreasen</i>	519
18.1 Introduction	519
18.2 Studying Fluctuation and Dissipation with FDTD	519
18.3 Introducing Blackbody Radiation into the FDTD Grid	520
18.4 Simulations in Vacuum	523
18.5 Simulations of an Open Cavity	526
18.5.1 Markovian Regime ($\tau \gg \tau_c$)	526
18.5.2 Non-Markovian Regime ($\tau \sim \tau_c$)	528
18.5.3 Analytical Examination and Comparison	530
18.6 Summary and Outlook	531
References	532

19 Casimir Forces in Arbitrary Material Geometries

Ardavan Oskooi and Steven G. Johnson

535

19.1	Introduction	535
19.2	Theoretical Foundation	536
19.2.1	Stress-Tensor Formulation	536
19.2.2	Complex Frequency Domain	537
19.2.3	Time-Domain Approach	538
19.2.4	Expression for the Casimir Force as a Time-Domain Integration	541
19.2.5	Evaluation of $g(-t)$ in (19.28)	542
19.3	Reformulation in Terms of a Harmonic Expansion	544
19.4	Numerical Study 1: A 2-D Equivalent to a 3-D Configuration	545
19.5	Numerical Study 2: Dispersive Dielectric Materials	548
19.6	Numerical Study 3: Cylindrical Symmetry in Three Dimensions	550
19.7	Numerical Study 4: Periodic Boundary Conditions	552
19.8	Numerical Study 5: Fully 3-D FDTD-Casimir Computation	553
19.9	Generalization to Nonzero Temperatures	556
19.9.1	Theoretical Foundation	556
19.9.2	Incorporating $T > 0$ in the Time Domain	557
19.9.3	Validations	558
19.9.4	Implications	559
19.10	Summary and Conclusions	560
	Acknowledgments	560
	Appendix 19A: Harmonic Expansion in Cylindrical Coordinates	561
	References	562

20 Meep: A Flexible Free FDTD Software Package

Ardavan Oskooi and Steven G. Johnson

567

20.1	Introduction	567
20.1.1	Alternative Computational Tools	568
20.1.2	The Initial-Value Problem Solved by Meep	568
20.1.3	Organization of This Chapter	569
20.2	Grids and Boundary Conditions	570
20.2.1	Coordinates and Grids	570
20.2.2	Grid Chunks and Owned Points	570
20.2.3	Boundary Conditions and Symmetries	572
20.3	Approaching the Goal of Continuous Space-Time Modeling	573
20.3.1	Subpixel Smoothing	573
20.3.2	Interpolation of Field Sources	576
20.3.3	Interpolation of Field Outputs	578
20.4	Materials	578
20.4.1	Nonlinear Materials	579
20.4.2	Absorbing Boundary Layers: PML, Pseudo-PML, and Quasi-PML	579
20.5	Enabling Typical Computations	581
20.5.1	Computing Flux Spectra	581
20.5.2	Analyzing Resonant Modes	582
20.5.3	Frequency-Domain Solver	583
20.6	User Interface and Scripting	586
20.7	Abstraction Versus Performance	588
20.7.1	Primacy of the Inner Loops	589
20.7.2	Time-Stepping and Cache Trade-Offs	589

20.7.3 The Loop-in-Chunks Abstraction	591
20.8 Summary and Conclusions	592
Acknowledgments	592
References	592
Acronyms and Common Symbols	597
About the Authors	601
Index	611

Preface

Advances in photonics and nanotechnology have the potential to revolutionize humanity's ability to communicate and compute, to understand fundamental life processes, and to diagnose and treat dread diseases such as cancer. To pursue these advances, it is crucial to understand and properly model the interaction of light with nanometer-scale, three-dimensional (3-D) material structures. Important geometric features and material inhomogeneities of such structures can be as small as a few tens of atoms laid side by side. Currently, it is recognized that the most efficient computational modeling of optical interactions with such nanoscale structures is based on the numerical solution of the fundamental Maxwell's equations of classical electrodynamics, supplemented as needed by spatially localized hybrids with (the even more fundamental, but computationally much more intense) quantum electrodynamics.

Aimed at academic and industrial researchers working in all areas of photonics and nanotechnology, this book reviews the current state-of-the-art in formulating and implementing computational models of optical interactions with nanoscale material structures. Maxwell's equations are solved using the finite-difference time-domain (FDTD) technique, investigated over the past 40 years primarily in the context of electrical engineering by one of us (Taflove),¹ and over the past 12 years primarily in the context of physics by two of us (Oskooi and Johnson).²

On one level, this book provides an update (for general applications) of the FDTD techniques discussed in the 2005 Taflove-Hagness Artech book, *Computational Electrodynamics: The Finite-Difference Time-Domain Method*, 3rd ed.³ (It is assumed that the readers of this book are familiar with the fundamentals of FDTD solutions of Maxwell's equations, as documented therein.) On another level, this book provides a wide-ranging review of recent FDTD techniques aimed at solving specific current problems of high interest in photonics and nanotechnology.

Chapters 1 through 7 of this book present important recent advances in FDTD and pseudospectral time-domain (PSTD) algorithms for modeling general electromagnetic wave interactions. Capsule summaries of these chapters follow.

Chapter 1: "Parallel-Processing Three-Dimensional Staggered-Grid Local-Fourier-Basis PSTD Technique," by M. Ding and K. Chen. This chapter discusses a new staggered-grid, local-Fourier-basis PSTD technique for efficient computational solution of the full-vector Maxwell's equations over electrically large, open-region, 3-D domains. The new PSTD formulation scales more efficiently with the size of the computational domain than previous collocated-grid PSTD approaches, and very importantly, *avoids the Gibbs phenomenon artifact*. This allows accurate

¹See the online article, <http://www.nature.com/milestones/milephotons/full/milephotons02.html>, in which *Nature Milestones/Photons* cites Prof. Taflove as one of the two principal pioneers of numerical methods for solving Maxwell's equations.

²Dr. Oskooi and Prof. Johnson have led the development of a powerful, free, open-source implementation of a suite of FDTD Maxwell's equations solvers at the Massachusetts Institute of Technology (MIT): *Meep* (acronym for MIT Electromagnetic Equation Propagation), available online at <http://ab-initio.mit.edu/meep>. Meep has been cited in over 600 journal publications, and has been downloaded more than 54,000 times.

³As of September 2012, the combined citations of the three editions (1995, 2000, and 2005) of *Computational Electrodynamics: The Finite-Difference Time-Domain Method*, rank this book 7th on the *Google Scholar*[®] list of the most-cited books in physics, according to the Institute of Optics of the University of Rochester. See: http://www.optics.rochester.edu/news-events/news/google_scholar.html.

PSTD modeling of dielectric structures having high-contrast material interfaces. The complete algorithm is presented, including its implementation for a uniaxial perfectly matched layer (UPML) absorbing boundary condition (ABC).

Chapter 2: “Unconditionally Stable Laguerre Polynomial-Based FDTD Method,” by B. Chen, Y. Duan, and H. Chen. This chapter discusses an efficient algorithm for implementing the unconditionally stable 3-D Laguerre polynomial-based FDTD technique with an effective PML ABC. In contrast to the conventional Laguerre-based FDTD method, which requires solving a very large sparse matrix, the new technique requires solving only six tri-diagonal matrices and three explicit equations for a full update cycle. This provides excellent computational accuracy — much better than alternating-direction-implicit FDTD approaches — and can be efficiently parallel-processed on a computing cluster.

Chapter 3: “Exact Total-Field/Scattered-Field Plane-Wave Source Condition,” by T. Tan and M. Potter. This chapter discusses an efficient exact FDTD total-field/scattered-field plane-wave source suitable for arbitrary propagation and polarization angles, stability factors, and non-unity aspect ratios. This technique provides *zero leakage* of the incident plane wave into the scattered-field region to machine-precision levels. The incremental computer memory and execution time are essentially negligible compared to the requirements of the primary 3-D grid.

Chapter 4: “Electromagnetic Wave Source Conditions,” by A. Oskooi and S. G. Johnson. This chapter provides a tutorial discussion of relationships between current sources and the resulting electromagnetic waves in FDTD simulations. The techniques presented are suitable for a wide range of modeling applications, from deterministic radiation, scattering, and waveguiding problems to nanoscale material structures interacting with thermal and quantum fluctuations. The chapter begins with a discussion of incident fields and equivalent currents, examining the principle of equivalence and the discretization and dispersion of equivalent currents in FDTD models. This is followed by a review of means to separate incident and scattered fields, whether in the context of scatterers, waveguides, or periodic structures. The next major topic is the relationship between current sources and the resulting local density of states. Here, key sub-topics includes the Maxwell eigenproblem and the density of states, radiated power and the harmonic modes, radiated power and the local density of states, computation of the local density of states in FDTD, Van Hove singularities in the local density of states, and resonant cavities and Purcell enhancement. Subsequent major topics include source techniques that enable covering a wide range of frequencies and incident angles in a small number of simulations for waves incident on a periodic surface; sources to efficiently excite eigenmodes in rectangular supercells of periodic systems; moving sources to enable modeling of Cherenkov radiation and Doppler-shifted radiation; and finally thermal sources via a Monte-Carlo/Langevin approach to enable modeling radiative heat transfer between complex-shaped material objects in the near field.

Chapter 5: “Rigorous PML Validation and a Corrected Unsplit PML for Anisotropic Dispersive Media,” by A. Oskooi and S. G. Johnson. This chapter discusses a straightforward technique to verify the correctness of any proposed PML formulation, irrespective of its implementation. Several published claims of working PMLs for anisotropic media, periodic media, and oblique waveguides are found to be just instances of adiabatic pseudo-PML absorbers. This chapter also discusses an efficient, corrected, unsplit PML formulation for anisotropic dispersive media, involving a simple refactorization of typical UPML proposals. Appendixes to this chapter provide a tutorial discussion of the complex-coordinate-stretching basis of PML, and the application of coupled-mode theory to analyze and design effective adiabatic pseudo-PML absorbers for FDTD modeling of photonic crystals.

Chapter 6: “Accurate FDTD Simulation of Discontinuous Materials by Subpixel Smoothing,” by A. Oskooi and S. G. Johnson. This chapter discusses an efficient local (“subpixel”) dielectric smoothing technique for achieving second-order accuracy when modeling non-grid-aligned isotropic and anisotropic dielectric interfaces in a Cartesian FDTD grid. This technique is based on a rigorous perturbation theory (summarized in an Appendix), rather than on an *ad hoc* heuristic. It provides greatly improved accuracy relative to previous approaches without increasing the required computational storage or running time. Subpixel smoothing has an additional benefit: it allows the simulation to respond continuously to changes in the geometry, such as during optimization or parameter studies, rather than changing in discontinuous jumps as dielectric interfaces cross pixel boundaries. Additionally, it yields much smoother convergence of the error with grid resolution, which makes it easier to evaluate the accuracy of a simulation, and enables the possibility of extrapolation to gain another order of accuracy. Unlike methods that require modified field-update equations or larger stencils and complicated position-dependent difference equations for higher-order accuracy, subpixel smoothing uses the standard center-difference expressions, and is easy to implement in FDTD by simply preprocessing the materials.

Chapter 7: “Stochastic FDTD for Analysis of Statistical Variation in Electromagnetic Fields,” by S. M. Smith and C. M. Furse. This chapter discusses a new stochastic FDTD (S-FDTD) technique that provides an efficient means to evaluate statistical variations in numerical simulations of electromagnetic wave interactions caused by random variations of the electrical properties of the model. The statistics of these variations are incorporated *directly* into FDTD, which computes an estimate of the resulting mean and variance of the fields at every point in space and time with a *single run*. The field variances computed using only two S-FDTD runs can effectively “bracket” the results using the brute-force Monte Carlo technique, the latter obtained after hundreds or thousands of runs. Hence, the S-FDTD technique offers a potentially huge savings in computation time, and opens up the possibility of assessing statistical parameters for applications in bioelectromagnetics, biophotonics, and geophysics where the material electrical properties have uncertainty or variability.

Chapters 8 through 20 provide a wide-ranging review of recent FDTD techniques aimed at solving specific current problems of high interest in photonics and nanotechnology. In order of presentation, the topics include:

- Plasmonics (emphasizing hybrid models with quantum mechanics), including active plasmonics, nonlocal electrodynamics, and modification of the optical properties of dye molecules closely bound to adjacent metal nanostructures
- Transformation electromagnetics, including non-diagonal anisotropic metamaterial cloaks
- Metamaterials, including periodic sub-wavelength optical structures comprised of non-rectangular-shaped plasmonic components
- Extensive tutorials on computational optical imaging for microscopy and nanoscale lithography
- Biophotonics applications, including imaging/characterization of intracellular structure and sensing of nanoscale intracellular anomalies indicative of early-stage cancer

- Non-paraxial spatial soliton propagation and interactions with nanoscale material structures
- Vacuum quantum phenomena, including blackbody radiation and electromagnetic fluctuations in dissipative open systems, and Casimir forces in arbitrary material geometries
- MIT's flexible, free FDTD software package, *Meep*.

Capsule summaries of these chapters follow.

Chapter 8: "FDTD Modeling of Active Plasmonics," by I. Ahmed, E. H. Khoo, and E. P. Li. This chapter discusses a recent hybrid FDTD/quantum mechanics technique for modeling plasmonic devices having integral semiconductor elements capable of providing gain upon pumping. The new technique integrates a Lorentz-Drude model to simulate the metal components of the device with a multi-level, multi-electron quantum model of the semiconductor component. Two examples of applications are summarized: amplification of a 175-fs optical pulse propagating in a thin, electrically pumped GaAs medium between two gold plates; and the resonance shift and radiation from a GaAs microcavity resonator with embedded gold nanocylinders. An appendix reviews the recent critical-points model for metal optical properties. This model is capable of providing a more accurate treatment of the bulk dielectric dispersion properties of various metals over a wider range of optical wavelengths than previously possible.

Chapter 9: "FDTD Computation of the Nonlocal Optical Properties of Arbitrarily Shaped Nanostructures," by J. M. McMahon, S. K. Gray, and G. C. Schatz. At length scales of less than ~ 10 nm, quantum-mechanical effects can lead to unusual optical properties for metals relative to predictions based on assuming bulk dielectric values. A full quantum-mechanical treatment of such nanostructures would be best, but is not practical for these structure sizes. However, it is possible to incorporate some quantum effects within classical electrodynamics via the use of a different dielectric model than that for the bulk metal. In this chapter, the quantum effect of primary interest requires a dielectric model wherein the material polarization at a point in space depends not only on the local electric field, but also on the electric field in its neighborhood. This chapter discusses a technique to calculate the optical response of an arbitrarily shaped nanostructure described by such a spatially nonlocal dielectric function. This technique is based on converting the hydrodynamic Drude model into an equation of motion for the conduction electrons, which then serves as a current field in the Maxwell-Ampere law. The latter is incorporated in a self-consistent manner in the FDTD solution of Maxwell's curl equations. Using this hybrid technique, modeling results for one-dimensional (1-D), two-dimensional (2-D), and 3-D gold nanostructures of variable size are presented. These results demonstrate the increasing importance of including nonlocal dielectric phenomena when modeling optical interactions with gold nanostructures as characteristic length scales of interest fall below ~ 10 nm.

Chapter 10: "Classical Electrodynamics Coupled to Quantum Mechanics for Calculation of Molecular Optical Properties: An RT-TDDFT/FDTD Approach," by H. Chen, J. M. McMahon, M. A. Ratner, and G. C. Schatz. This chapter discusses a new multiscale computational methodology to incorporate the scattered electric field of a plasmonic nanoparticle into a quantum-mechanical optical property calculation for a nearby dye molecule. For a given location of the dye molecule with respect to the nanoparticle, a frequency-dependent scattering response function is first computed using FDTD. Subsequently, the time-dependent scattered electric field at the dye molecule is calculated using this response function through a multidimensional Fourier transform to reflect the effect of polarization of the nanoparticle on the

local field at the dye molecule. Finally, a real-time time-dependent density function theory (RT-TDDFT) approach is employed to obtain the desired optical property of the dye molecule in the presence of the nanoparticle's local electric field. Using this technique, enhanced absorption spectra of the N3 dye molecule and enhanced Raman spectra of the pyridine molecule are modeled, assuming proximity to a 20-nm-diameter silver nanosphere. The computed signal amplifications reflect the strong coupling between the wavelike response of the dye molecule's individual electrons and the collective action of the silver nanosphere's dielectric medium. Overall, this hybrid method provides a bridge spanning the gap between quantum mechanics and classical electrodynamics (i.e., FDTD) with respect to both length and time scales.

Chapter 11: "Transformation Electromagnetics Inspired Advances in FDTD Methods," by R. B. Armenta and C. D. Sarris. Transformation electromagnetics exploits the coordinate-invariance property of Maxwell's equations to synthesize the permeability and permittivity tensors of artificial materials to guide electromagnetic waves in specified manners. This chapter shows how employing a coordinate system-independent representation of Maxwell's equations based on the invariance principle provides powerful additional FDTD capabilities, including conformal modeling of curved material boundaries, incorporation of artificial materials providing novel wave-propagation characteristics, and time-dependent discretizations for high-resolution tracking of moving electromagnetic pulses. Examples of these enhanced FDTD capabilities are derived from coordinate transformations of Maxwell's equations involving projections onto the covariant-contravariant vector bases associated with a general curvilinear coordinate system.

Chapter 12: "FDTD Modeling of Non-Diagonal Anisotropic Metamaterial Cloaks," by N. Okada and J. B. Cole. Without proper care, the direct application of FDTD to simulate transformation-based metamaterials having non-diagonal anisotropic constitutive parameters is prone to numerical instabilities. This chapter discusses the basis, formulation, and validation of a technique to solve this instability problem by ensuring that the numerically derived FDTD equations are exactly symmetric. The crucial step in this technique involves finding the eigenvalues and diagonalizing the constitutive tensors. After this diagonalization, any of the previously reported FDTD algorithms for purely diagonal metamaterial cases can be applied. The technique is illustrated with a 2-D FDTD model of a transformation-based elliptical cylindrical cloak comprised of a non-diagonal anisotropic metamaterial. The cloak is found to greatly reduce both the bistatic radar cross-section and the total scattering cross-section of the enclosed elliptical perfect electric conductor (PEC) cylinder at the design wavelength. In fact, as the grid of the FDTD model is progressively refined, scattering by the cloaked PEC cylinder trends rapidly toward zero. However, the bandwidth of the effective scattering reduction is only ~4%; so narrow that it may be described as just a scattering null. This narrow bandwidth appears to limit practical applications of such cloaks.

Chapter 13: "FDTD Modeling of Metamaterial Structures," by Costas D. Sarris. This chapter provides an overview of the application of FDTD to several key classes of problems in metamaterial analysis and design, from two complementary perspectives. First, FDTD analyses of the transient response of several metamaterial structures of interest are presented. These include negative-refractive-index media and the "perfect lens," an artificial transmission line exhibiting a negative group velocity, and a planar anisotropic grid supporting resonance cone phenomena. Second, periodic geometries realizing metamaterial structures are studied. The primary tool used here is the sine-cosine method, coupled with the array-scanning technique. This tool is applied to obtain the dispersion characteristics (and, as needed, the electromagnetic field) associated with planar periodic positive-refractive-index and negative-refractive-index

transmission lines, as well as the planar microwave “perfect lens” comprised of sections of 2-D transmission lines exhibiting both positive and negative equivalent refractive indices. The chapter continues with a review of the triangular-mesh FDTD technique for modeling optical metamaterials with plasmonic components, and how this technique could be coupled with the sine-cosine method to analyze periodic plasmonic microstructures requiring much better modeling of slanted and curved metal surfaces than is possible using a Cartesian FDTD grid and simple staircasing. Finally, the periodic triangular-mesh FDTD technique is applied to accurately obtain the dispersion characteristics and electromagnetic modes of a sub-wavelength plasmonic photonic crystal comprised of an array of silver microcylinders.

Chapter 14: “Computational Optical Imaging Using the Finite-Difference Time-Domain Method,” by I. R. Capoglu, J. D. Rogers, A. Taflove, and V. Backman. This chapter presents a comprehensive and rigorous tutorial discussion of the theoretical principles that comprise the foundation for emerging electromagnetic-field models of optical imaging systems based on 3-D FDTD solutions of Maxwell’s curl equations. These models provide the capability to computationally synthesize images formed by *every* current form of optical microscopy (bright-field, dark-field, phase-contrast, etc.), as well as optical metrology and photolithography. Focusing, variation of the numerical aperture, and so forth can be adjusted simply by varying a few input parameters – literally a *microscope in a computer*. This permits simulations of both existing and proposed novel optical imaging techniques over a 10^7 :1 dynamic range of distance scales, i.e., from a few nanometers (the FDTD voxel size within the microstructure of interest) to a few centimeters (the location of the image plane where the amplitude and phase spectra of individual pixels are calculated). This tutorial shows how a general optical imaging system can be segmented into four self-contained sub-components (illumination, scattering, collection and refocusing), and how each of these sub-components is mathematically analyzed. Approximate numerical methods used in the modeling of each sub-component are explained in appropriate detail. Relevant practical applications are cited whenever applicable. Finally, the theoretical and numerical results are illustrated via several implementation examples involving the computational synthesis of microscope images of micro-scale structures. Overall, this chapter constitutes a useful starting point for those interested in modeling optical imaging systems from a rigorous electromagnetic-field point of view. A distinct feature of this approach is the extra attention paid to the issues of discretization and signal processing – a key issue in finite methods such as FDTD, where the electromagnetic field is only computed at a finite set of spatial and temporal points.

Chapter 15: “Computational Lithography Using the Finite-Difference Time-Domain Method,” by G. W. Burr and J. T. Azpiroz. This chapter presents a comprehensive and rigorous tutorial discussion of the fundamental physical concepts and FDTD numerical considerations whose understanding is essential to perform electromagnetic-field computations for very large-scale integration (VLSI) optical lithography in the context of semiconductor microchip manufacturing. As the characteristic dimensions of VLSI technology shrink and complexity increases, the usual geometrical approximations of the electromagnetic field interactions underlying optical lithographic technology can become increasingly inaccurate. However, the accurate simulation of both immersion and extreme ultraviolet (EUV) lithographic systems is expected to be an increasingly critical component of semiconductor manufacturing for the foreseeable future. While rigorous computations of the required 3-D electromagnetic fields can be much slower than approximate methods, rapid turnaround is still crucial. The FDTD method offers advantages such as flexibility, speed, accuracy, parallelized computation, and the ability to

simulate a wide variety of materials. In fact, FDTD computation of the electromagnetic fields underlying VLSI optical lithography currently offers the best combination of accuracy and turn-around time to understand and model field effects involved with relatively small patterns.

Chapter 16: “FDTD and PSTD Applications in Biophotonics,” by I. R. Capoglu, J. D. Rogers, C. M. Ruiz, J. J. Simpson, S. H. Tseng, K. Chen, M. Ding, A. Taflove, and V. Backman. This chapter discusses qualitatively the technical basis and representative applications of FDTD and PSTD computational solutions of Maxwell’s curl equations in the area of biophotonics. The FDTD applications highlighted in this chapter reveal its ability to provide ultrahigh-resolution models of optical interactions within individual biological cells, and furthermore to provide the physics kernel of advanced computational microscopy techniques. The PSTD applications highlighted in this chapter indicate its ability to model optical interactions with clusters of many biological cells and even macroscopic sections of biological tissues, especially in regard to developing an improved understanding of the physics of enhanced optical backscattering and turbidity suppression. In all of this, a key goal is to inform readers how FDTD and PSTD can put Maxwell’s equations to work in the analysis and design of a wide range of biophotonics technologies. These technologies exhibit promise to advance the basic scientific understanding of cellular-scale processes, and to provide important medical applications (especially in early-stage cancer detection).

Chapter 17: “GVADE FDTD Modeling of Spatial Solitons,” by Z. Lubin, J. H. Greene, and A. Taflove. The general vector auxiliary differential equation (GVADE) FDTD method, discussed in this chapter, is a powerful tool for first-principles, full-vector solutions of electromagnetic wave interactions in materials having combined linear and nonlinear dispersions. This technique provides a direct time-domain solution of Maxwell’s curl equations without any simplifying paraxial, slowly varying envelope, or scalar approximations. Furthermore, it can be applied to arbitrary inhomogeneous material geometries, and both linear and nonlinear polarizations can be incorporated through the Maxwell-Ampere law. This chapter derives the GVADE FDTD time-stepping algorithm for the electromagnetic field in a realistic 2-D model of fused silica characterized by a three-pole Sellmeier linear dispersion, an instantaneous Kerr nonlinearity, and a dispersive Raman nonlinearity. (Here, the electric field is assumed to have both a longitudinal and a transverse component in the plane of incidence.) Next, the technique is extended to model a plasmonic metal characterized by a linear Drude dispersion. The GVADE FDTD method is then applied to model the propagation of single nonparaxial and overpowered spatial solitons; the interaction of a pair of closely spaced, co-propagating, nonparaxial spatial solitons; spatial soliton scattering by subwavelength air holes; and interactions between nonparaxial spatial solitons and thin gold films. It is concluded that the GVADE FDTD technique will find emerging applications in optical communications and computing involving micro- and nano-scale photonic circuits that require controlling complex electromagnetic wave phenomena in linear and nonlinear materials with important subwavelength features.

Chapter 18: “FDTD Modeling of Blackbody Radiation and Electromagnetic Fluctuations in Dissipative Open Systems,” by J. Andreasen. This chapter discusses how the FDTD method can simulate fluctuations of electromagnetic fields in open cavities due to output coupling. The foundation of this discussion is the fluctuation-dissipation theorem, which dictates that cavity field dissipation by leakage is accompanied by thermal noise, simulated here by classical electrodynamics. The absorbing boundary of the FDTD grid is treated as a blackbody that radiates into the grid. Noise sources are synthesized with spectra equivalent to that of blackbody radiation at various temperatures. When an open dielectric cavity is placed in the FDTD grid,

the thermal radiation is coupled into the cavity and contributes to the thermal noise for the cavity field. In the Markovian regime, where the cavity photon lifetime is much longer than the coherence time of thermal radiation, the FDTD-calculated amount of thermal noise in a cavity mode agrees with that given by the quantum Langevin equation. This validates the numerical model of thermal noise that originates from cavity openness or output coupling. FDTD simulations also demonstrate that, in the non-Markovian regime, the steady-state number of thermal photons in a cavity mode exceeds that in a vacuum mode. This is attributed to the constructive interference of the thermal field inside the cavity. The advantage of the FDTD numerical model is that the thermal noise is added in the time domain without any prior knowledge of cavity modes. Hence, this technique can be applied to simulate complex open systems whose modes are not known prior to the FDTD calculations. This approach is especially useful for very leaky cavities whose modes overlap strongly in frequency, as the thermal noise related to the cavity leakage is introduced naturally without distinguishing the modes. Therefore, the method discussed here can be applied to a wide range of quantum optics problems.

Chapter 19: “Casimir Forces in Arbitrary Material Geometries,” by A. Oskooi and S. G. Johnson. This chapter discusses how FDTD modeling provides a flexible means to compute Casimir forces for essentially arbitrary configurations and compositions of micro- and nanostructures. Unlike other numerical techniques proposed for this application, FDTD is not structure specific, and hence, very general codes such as MIT’s freely available *Meep* software (Chapter 20) can be used with no modifications. The chapter begins by establishing the theoretical foundation for the FDTD-Casimir technique. This is followed by a discussion of an efficient implementation employing a rapidly convergent harmonic expansion in the source currents. Then, means to extend the FDTD-Casimir technique to account for nonzero temperatures are presented. The chapter provides five FDTD-Casimir modeling examples, concluding with a fully 3-D simulation where the Casimir force transitions from attractive to repulsive depending on a key separation parameter. Overall, in addition to providing simulations of fundamental physical phenomena, these developments in FDTD-Casimir modeling may permit the design of novel micro- and nano-mechanical systems comprised of complex materials.

Chapter 20: “Meep: A Flexible Free FDTD Software Package,” by A. Oskooi and S. G. Johnson. This chapter discusses aspects of the free, open-source implementation of the FDTD algorithm developed at the Massachusetts Institute of Technology (MIT): *Meep* (acronym for MIT Electromagnetic Equation Propagation), available online at <http://ab-initio.mit.edu/meep>. *Meep* is a full-featured software package, including, for example, arbitrary anisotropic, nonlinear, and dispersive electric and magnetic media modeling capabilities; a variety of boundary conditions including symmetries and PMLs; distributed-memory parallelism; spatial grids in Cartesian coordinates in one, two, and three dimensions as well as in cylindrical coordinates; and flexible output and field computations. *Meep* also provides some unusual features: advanced signal processing to analyze resonant modes; subpixel smoothing to accurately model slanted and curved dielectric interfaces in a Cartesian grid; a frequency-domain solver that exploits the time-domain code; complete scriptability; and integrated optimization facilities. This chapter begins with a discussion of the fundamental structural unit of “chunks” that constitute the FDTD grid and enable parallelization. Next, an overview is provided of *Meep*’s core design philosophy of approaching the goal of continuous space-time modeling for inputs and outputs. The discussion continues with an explanation and motivation of *Meep*’s somewhat-unusual design intricacies for nonlinear materials and PMLs; important aspects of *Meep*’s computational methods for flux spectra and resonant modes; a demonstration

of the formulation of Meep’s frequency-domain solver that requires only minimal modifications to the underlying FDTD algorithm; and how Meep’s features are accessible to users via a scripting interface. Overall, a free/open-source, full-featured FDTD package like Meep can play a vital role in enabling new research in electromagnetic phenomena. Not only does it provide a low barrier to entry for standard FDTD simulations, but the simplicity of the FDTD algorithm combined with access to the Meep source code offers an easy route to investigate new physical phenomena coupled with classical electrodynamics.

Acknowledgments

We gratefully acknowledge all of our contributing chapter authors. Their biographical sketches appear in the “About the Authors” section. And of course, we acknowledge our respective family members who exhibited great patience and kept their good spirits during the development of this book.

Allen Taflove, Evanston, Illinois

Ardavan Oskooi, Kyoto, Japan

Steven G. Johnson, Cambridge, Massachusetts

November 2012